Computational Fluid Dynamics-Based Study of an Oilfield Separator—Part II: An Optimum Design

Ali Pourahmadi Laleh and **William Y. Svrcek,** University of Calgary, and **Wayne D. Monnery,** Chem-Pet Process Tech Limited

Summary

This paper provides details of comprehensive computational-fluid-dynamics (CFD) -based studies performed to overcome the separation inefficiencies experienced in a large-scale three-phase separator. It will be shown that the classic design methods are too conservative and would result in oversized separators. In this study, effective CFD models are developed to estimate the phase-separation parameters that are integrated into an algorithmic design method to specify a realistic optimum separator. The CFD simulations indicated that noticeable residence times are required for liquid droplets to penetrate through the interfaces, and liquid droplets would be entrained again from the liquid/liquid-interface vicinity by the continuous liquid phase.

Introduction

The main purpose of the surface facilities on an oil-production platform is to separate the produced multiphase stream into its vapor and liquid fractions. In fact, a properly sized primary multiphase separator can increase the capacity of the entire facility. The literature on the critical unit operation of multiphase separators is extensive, particularly regarding two-phase separators. Most of these documents propose separator-design guidelines and some address operating-performance issues associated with multiphase separators. In a very few studies, CFD-based simulations have been performed to provide a realistic picture of fluid-phase-separation phenomena and to improve separator efficiency. These CFD-based studies, however, have been focused generally on performance issues in specific operating separators. Recently, a realistic CFD simulation of an oilfield three-phase separator has been provided by Pourahmadi Laleh et al. (2012). The separator of interest was installed on the Gullfaks-A offshore platform. The original CFD-based study of this separator was performed by Hansen et al. (1993), and the paper provided the geometrical specifications of the Gullfaks-A separator **(Fig. 1)** and the physical parameters for the fluids **(Table 1).**

Production on the Gullfaks-A platform started in 1986–87, and the separator performed as expected during the first years. However, several separation inefficiencies, such as emulsion problems and water-level-control failure, were experienced with increasing produced water-flow rate. The developed CFD simulation of the separator could capture these field-separation problems by evaluating the mass distribution of oil and water droplets between oil and water outlets. As presented in Pourahmadi Laleh et al. (2012), the overall separation efficiency of 98.0% in 1988 would decrease to 70.4% for the future-production condition. The separation efficiencies for oil and water droplets were calculated to be 100 and 96.9%, respectively, for the 1988 production condition. For the future-production condition, the separation efficiency was 1.3% for oil droplets and 100% for water droplets. Hence, it was concluded that major separation inefficiency would be encountered by the existing separator for the projected increase in the produced-water-flow rate.

To overcome the separation inefficiencies, various strategies will be presented in this paper. First, the effect of minor modifications such as adjusting the position and size of the flow-distributing baffles and changing the liquid levels will be examined. Then, a new separator will be designed using classic design methods, and its separation performance will be verified by CFD simulation. Finally, CFD-simulation results will be integrated into an algorithmic optimum-design method to specify a realistic separator for the Gullfaks-A process. For all the CFD case studies, generation of the physical model and the grid system was completed in the Gambit 2.4.6 (ANSYS 2006b) environment, and the CFD simulations were performed in the Fluent 6.3.26 (ANSYS 2006a) environment. The modeling strategies are the same as those of the preceding study and were discussed in Pourahmadi Laleh et al. (2012).

Minor Modifications

The first modification that was tested was adjusting the position of the distribution baffles. To test this effect, all the baffles were removed from the model to see if any tangible effect on the separator performance might be observed. With this change, the separation efficiency was calculated as 99.5% for oil droplets and 96.8% for water droplets at the 1988 production conditions and 0.8% for oil droplets and 100% for water droplets at the future-production conditions. Compared with the reported values for the separator equipped with the baffles, a negligible difference is seen. On the other hand, as concluded by Lu et al. (2007) in their CFD-based study, it can be expected that the baffles will improve the quality of liquid-flow distribution in the vessel and increase the separation efficiency.

Noting that the baffles were installed originally in the upper (vapor-disengagement) section of the separator, it would seem that some improvement might be achieved by expanding the baffles so that they cover the lower areas also. To investigate this issue, baffles in the inefficient operating separator were expanded to cover the entire cross-sectional area. The CFD simulation of droplet dispersions within the separator resulted in separation efficiencies of 0.5 and 100% for oil and water droplets, respectively. Therefore, it can be concluded that adjusting the arrangement of distributing baffles did not affect the separation efficiency in the Gullfaks-A separator significantly. In fact, as emphasized by Lyons and Plisga (2005), although properly designed internals are generally helpful in reducing liquid carryover at design conditions, they cannot overcome separation problems in a basically inefficient design or in an undersized separator.

The other modification analyses were performed by changing the liquid levels. Although the separation efficiency remained approximately 100% for the water droplets in all the liquid-level anal-

Original SPE manuscript received for review 29 November 2011. Revised manuscript received for review 10 February 2012. Paper (SPE 161036) peer approved 15 March 2012.

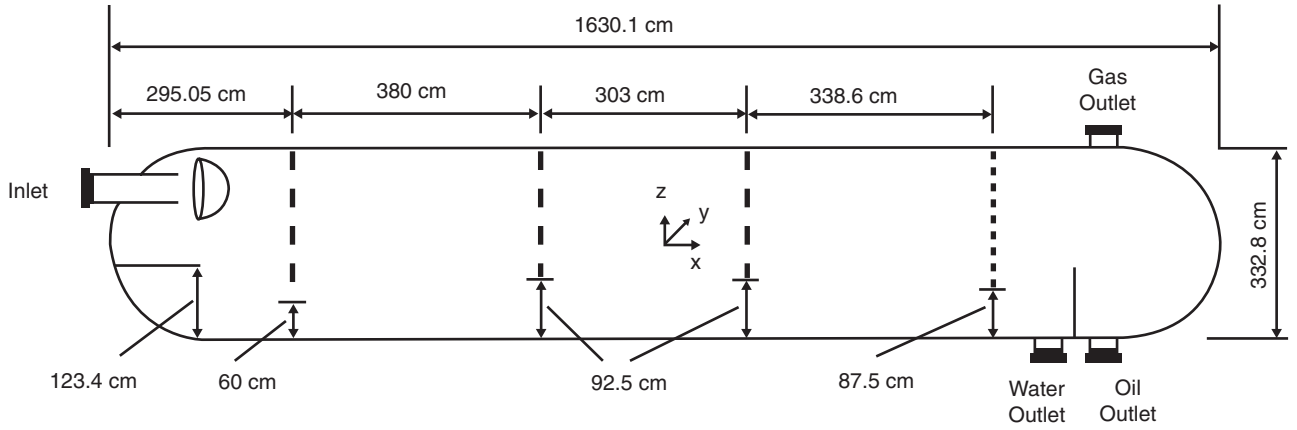

Fig. 1—Geometrical specifications of the Gullfaks-A separator (Hansen et al. 1993).

yses studied, the separation efficiency for the oil droplets generally decreased to

- 0.08% with an increase of 20 cm in the thickness of the water layer
- 0.03% with a decrease of 20 cm in the thickness of the water layer
- 0.02% with an increase of 20 cm in thickness of both the water and oil layers

Thus, it may be concluded from the CFD simulations that minor modifications cannot change the separation inefficiencies in the Gullfaks-A separator, and this separator should be redesigned to perform the phase-separation task successfully at projected produced-water-flow rates.

Redesign of the Gullfaks-A Separator

Multiphase separators are designed to provide sufficient disengagement space for gas/liquid phases and adequate retention time for liquid phases to establish satisfactory liquid/liquid separation. Some heuristics have been suggested in the literature that are usually conservative and lead to oversized separators (Abernathy 1993). In more-systematic procedures, droplet-settling theory is applied for evaluating vapor/liquid- or liquid/liquid-separation requirements, and adequate retention times may be assumed on the basis of experience, scale-model predictions, or field data. Grødal and Realff (1999) developed a software package for automatic design of two-phase and three-phase separators. The design procedure was based on droplet-settling theory, and the optimum solution was determined by applying sequential quadratic-programming techniques.

As stated by Grødal and Realff (1999), the most-comprehensive approach among the classic methods was proposed by Svrcek and Monnery (Svrcek and Monnery 1993; Monnery and Svrcek 1994). In their approach, an algorithmic method was developed on the basis of accepted industrial guidelines, and the optimum (most-economical) multiphase separator was designed through iteration (for horizontal separators) or height adjustment (for vertical separators). To provide more details of the approach, the main steps used in designing the "weir-" type three-phase separator proposed by Monnery and Svrcek (1994) are presented in Appendix A.

Redesign of the Gullfaks-A Separator on the Basis of the Classic Methods. The algorithmic-design method proposed by Monnery and Svrcek (1994) was used in redesigning the Gullfaks-A separator. The method uses industry-standard settling or rising velocities to design the most-economical separator. Unfortunately, the exact values of settling or rising velocities of droplets may be totally different from the industry-accepted values. The usual value for liquid-droplet size is 150 μm and is used as a standard in the American Petroleum Institute (API) design method (Walas 1990; Hooper 1997). However, assuming this droplet size, no realistic results could be obtained for the Gullfaks-A separator. That is, a separator with a diameter of 14.4 m and a length of 87 m would result for separating the mixture at 1988 production conditions, and a separator with dimensions of 12.4 m×75 m would result for the future-water-production conditions.

The calculated separator dimensions imply that, through classic design strategy, there is no feasible design for separating the mixture with the Gullfaks-A production conditions. However, both CFD-simulation results and the oilfield experience showed that the original separator did operate in an acceptable way for the 1988 production conditions, and that the separation inefficiencies are a result of the increase in the produced-water-flow rate at the future-production conditions. This would imply that an acceptable design could be made by providing the liquid-retention times of the 1988-production conditions for the liquid phases at the increased flow rates. As noted by Svrcek and Monnery (1993), although the basic equations used for separator sizing are known widely, subjectivity exists during the selection of the parameters used in these equations. The most-controversial parameters are settling (or rising) velocities of droplets in liquid/liquid separation. These parameters are to be tuned using the 1988 production conditions, at which the separation efficiencies were acceptable.

Estimation of Settling Velocity of Oil Droplets in the Gas Phase. Two industrial methods—the Gas Processors Suppliers As-

TABLE 1—THE PHYSICAL PARAMETERS OF FLUIDS IN THE GULLFAKS-A SEPARATOR, PROVIDED BY HANSEN ET AL. (1993)

	1988 Production Rate (m^3/h)	Future Production Rate (m^3/h)	Density (kg/m^3)	Viscosity (Pa·s)
Gas	1640	1640	49.7	1.30E–5
Oil	1840	1381	831.5	5.25E–3
Water	287	1244	1030	4.30E–4
Operating Conditions	Temperature=55.4 °C and Pressure= 6870 kPa			

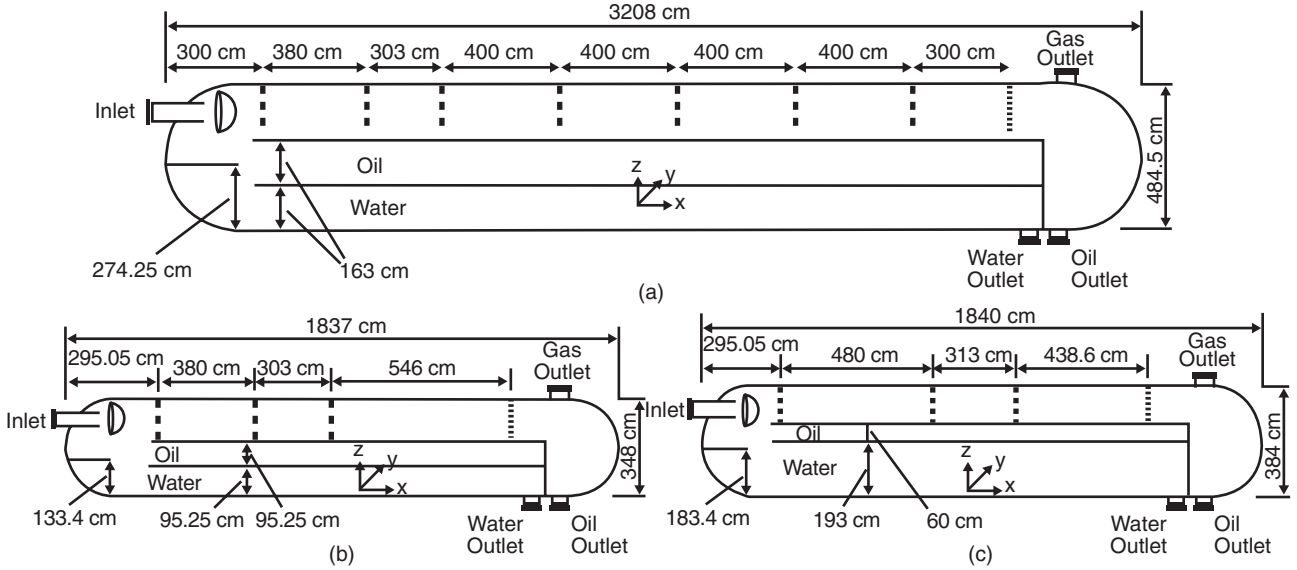

Fig. 2—Geometrical specifications of the modified separators for Gullfaks-A: (a) redesigned, (b) weir, and (c) stabilized.

sociation (GPSA 1998) method and the York-demister method—and one theoretical method were evaluated. Using these methods, the terminal settling velocity of oil droplets was calculated to be 0.460, 0.328, and 0.216 m/s, respectively. Thus, the corresponding minimum length required for the vapor/liquid separation in the original separator was calculated as 0.51, 0.71, and 1.08 m, respectively. The CFD simulations indicated that approximately 10 cm after the momentum breaker, almost all the liquid droplets had settled, implying that the calculated values are somewhat conservative. However, while sizing the Gullfaks-A separator, the classic procedure did indicate that the liquid/liquid separation is controlling. Therefore, the focus of the current phase of this study is on the proper estimation of oil/water-separation velocities.

Estimation of the Rising Velocity of Oil Droplets in the Water Phase. By use of the Stokes' law, a velocity of 0.00566 m/s was calculated for the industry-accepted droplet size of 150 μm. This value is greater than the value implied by the liquid-retention time, as follows. The separation efficiency of 100% for oil droplets indicates an appropriate separator design/size, and the retention time of this original separator was 165.6 seconds for water phase with a water-layer thickness of 0.625 m; hence, the rising velocity of oil droplets was assumed to be 0.00377 m/s while redesigning the separator.

Estimation of the Settling Velocity of Water Droplets in the Oil Phase. A velocity of 0.000464 m/s was calculated by Stokes' law, assuming a liquid-droplet size of 150 μm. In terms of the liquid-retention time theory, this value is too conservative and leads to an oversized separator. The installed separator with dimensions of 3.33 m×16.30 m had been working efficiently for the designed 1988 production conditions. The predicted separation efficiency of 96.9% for water droplets indicates that the design was successful in having the water droplets separated from the oil phase. Therefore, the provided retention time of 73.4 seconds for oil phase was reasonable. Accounting for the oil-layer thickness of 1.039 m, the settling velocity of water droplets should be 0.01416 m/s. To further improve the water-separation efficiency, a value of 0.0134 m/s (95% of 0.01416 m/s) was assumed while redesigning the separator.

Instead of the estimated values calculated from Stokes' law, new "separation velocities" were calculated on the basis of the appropriate liquid-retention time of the 1988-production condition. To specify a useable separator, the separator was redesigned for the maximum flow rates of produced gas, oil, and water.

Fig. 2a provides the sizing specifications of the "redesigned" Gullfaks-A separator. As expected, a larger separator is required. To keep the design in line with the original separator, four extra baffles with gaps of 4.0 m between them were also added to the new separator design. Then, a CFD model was developed for the redesigned separator to study its performance while processing the Gullfaks-A produced multiphase. The global quality of the produced mesh systems in terms of number of cells, maximum cell squish, cell skewness, and maximum aspect ratio is presented in **Table 2**, which

TABLE 2—QUALITY OF THE MESH SYSTEMS PRODUCED IN THE GAMBIT 2.4.6 (ANSYS 2006b) ENVIRONMENT FOR THE GULLFAKS-A SEPARATOR

	Number of Cells	Maximum Squish	Maximum Skewness	Maximum Aspect Ratio
Redesigned	1155813	0.961646	0.999632	128.621
Weir	985834	0.735457	0.895869	44.4761
Stabilized	966574	0.746627	0.895882	44.5911

Skewness of the Produced Mesh

Skewness Range		0-0.20	0.20-0.40	0.40-0.60	0.60-0.80	0.80-1.0
Cell Density	Redesigned	76.4772%	17.8354%	4.4223%	1.2607%	0.0044%
	Weir	80.1525%	14.9260%	3.4968%	1.4233%	0.0014%
	Stabilized	79.8406%	15.0993%	3.5702%	1.4884%	0.0015%

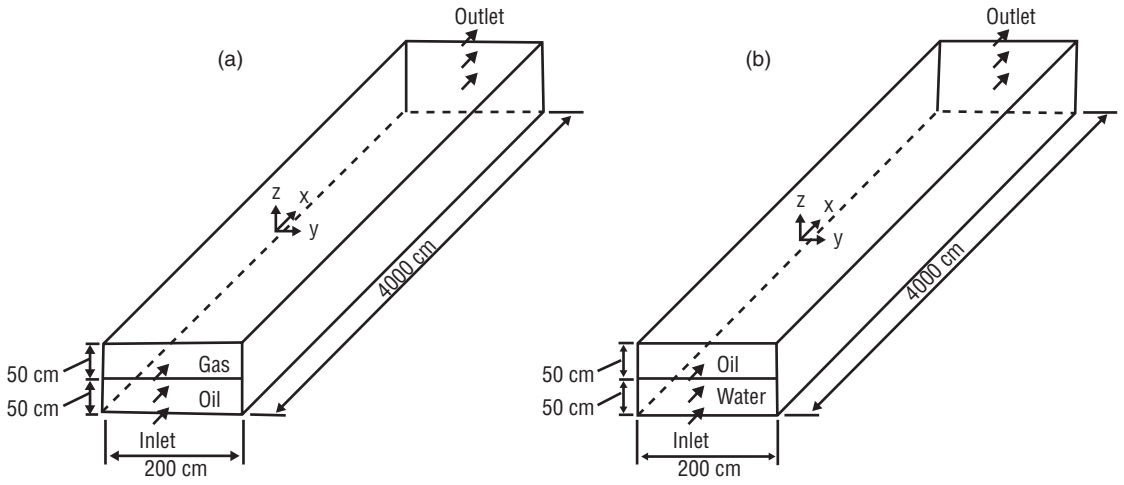

Fig. 3—The two-phase models developed for CFD simulation of phase separation: (a) vapor/liquid separation and (b) liquid/liquid separation.

does indicate that only a negligible fraction of cells (approximately 0.0044%) were of poor quality for this case.

Having set all the CFD parameters for the redesigned separator, approximately 5,100 iterations are required for continuous phase-solution convergence. Each iteration takes approximately 31 seconds, and a personal-computer (PC) run time of approximately 44 hours is required per solution of the continuous phases. A further PC run time of approximately 4 hours is also required for simulation of interactions between the dispersed droplets and continuous phases.

The modifications made as a result of the CFD simulation of this study did enhance the separator performance. The redesigned separator dealt satisfactorily with 1988 production conditions in that the total separation efficiency was as high as 99.1% (slightly higher than the original separator efficiency), with its components of 100 and 98.7% as separation efficiencies for oil and water droplets, respectively. For the projected future-production conditions, the redesigned separator had a total separation efficiency of 99.7%, with its components of 93.4 and 100% as separation efficiencies for oil and water droplets, respectively. Note that although approximately 6.6 wt% of the oil droplets was predicted to exit in the water outlet for the future-production case, this would not decrease the separated-water purity dramatically because the water-outlet composition would be 99.7% water and only 0.3% oil. As was the case with the original separator, there would be no droplet carryover in the gas-phase outlet (i.e., all the injected droplets exited in either the oil outlet or the water outlet).

CFD-Based Redesign of the Gullfaks-A Separator. To model the phase-separation process efficiently, two independent sets of CFD simulations were performed—one for vapor/liquid separation and the other for liquid/liquid separation. For this purpose, two two-phase models, shown in **Fig. 3,** were used. These models were developed by verification of the results for various two-phase systems when compared with those of industrial-scale separators. These investigations confirmed that although the mesh-generation stages in the Gambit environment and the setting of CFD parameters in the Fluent environment would be more straightforward for these models, the results produced for phase separations are the same as those for large-scale separators.

A sensitivity analysis on the defined droplet-size distribution showed that separation efficiencies are not overly sensitive to the assumed maximum droplet size (Pourahmadi Laleh 2010). Therefore, the required particle-size-distribution parameters were set as estimated for the 1988 production condition (Pourahmadi Laleh et al. 2012). The results are presented in **Table 3.** Note that in the developed models, for the first time, a distribution of droplets is being tracked. Therefore, to evaluate the separation velocities, a mass-averaged time taken by droplets to separate out of the continuous phases was used. So, the reported values are the "efficient" separation velocities.

Vapor/Liquid Separation. A settling velocity of 0.4967 m/s was calculated for oil droplets on the basis of the CFD simulations. This value is approximately 8% greater than the maximum terminal settling velocity estimated by the classic design methods (the GPSA method). However, CFD simulation showed that oil droplets required a residence time of 58 seconds to pass through the vapor/liquid interface. This is in contrast with the classic design methods, which assume that when oil or water droplets come into contact with vapor/liquid or liquid/liquid interfaces, they penetrate the interface immediately and join their respective phases.

As expected, water droplets with a settling velocity of 0.7055 m/s and an interface-residence time of 5.9 seconds required less time for separation from the gas phase compared with oil droplets.

Liquid/Liquid Separation. A rising velocity of 0.03002 m/s was calculated for oil droplets on the basis of CFD simulations. This value is approximately 4.3 times greater than the terminal rising velocity estimated by the classic design methods. However, similar to vapor/liquid separation, a noticeable residence time of 27.7 seconds was required for oil droplets to pass through the liquid/liquid interface.

For water droplets, a settling velocity of 0.01813 m/s was calculated. This value is approximately 38 times greater than the value estimated by the classic methods. Water droplets required only 2.7 seconds to penetrate through the liquid/liquid interface. Therefore, the classic design methods are too conservative when estimating the settling velocity for water droplets.

Having developed realistic separation parameters using CFD modeling, the algorithmic design method of Monnery and Svrcek (1994) was used to specify the most-economical separator. Their

TABLE 3—THE DISCRETE-PHASE PARAMETERS USED IN CFD SIMULATIONS OF PHASE SEPARATION

Discrete Phase Parameters	Oil Droplets	Water Droplets
Minimum Diameter (m)	100	100
Maximum Diameter (m)	2267	4000
Mean Diameter (m)	907	1600
Total Mass Flow-Rate (kg/s)	6.5E–4	4.4E–3
Number of Tracked Particles	1000	1000
Spread Parameter	2.6	2.6

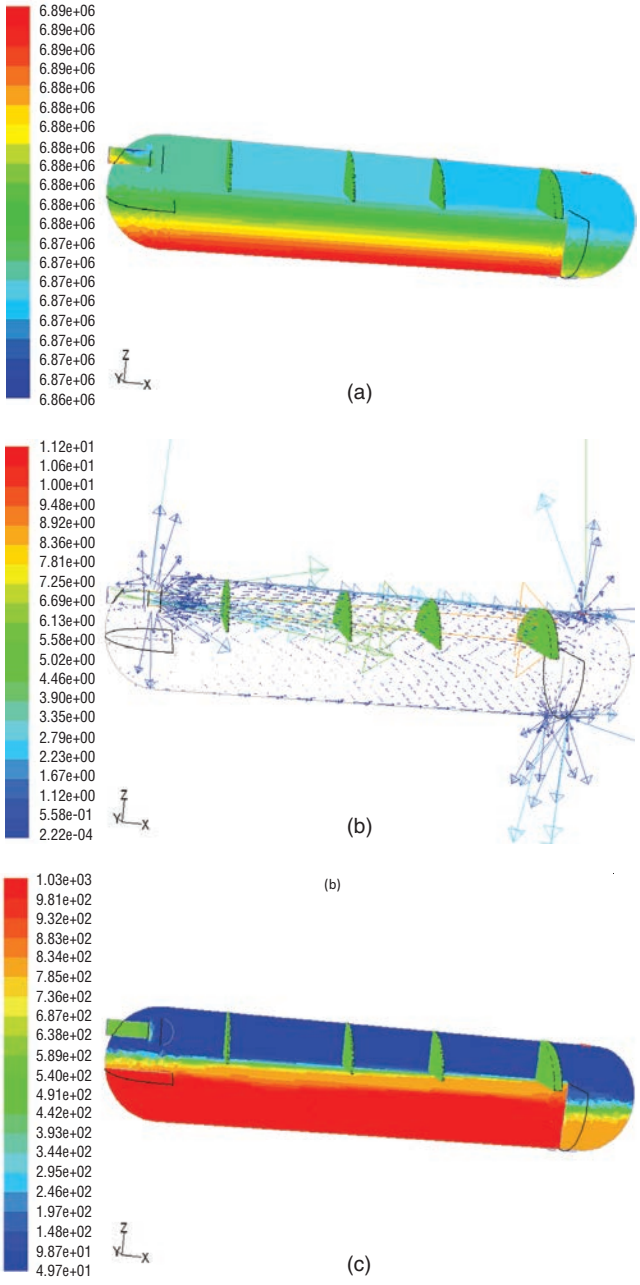

Fig. 4—Fluid-flow profiles in the middle of the stabilized separator designed for Gullfaks-A in the future-production conditions: (a) contours of pressure (Pa), (b) vectors of velocity (m/s), and (c) contours of density (kg/m^3).

design procedure used the separation velocities and interface-residence times obtained from the CFD simulations. Again, the maximum flow rates of the produced gas, oil, and water phases were used in the design.

Fig. 2b. presents the dimensions of the weir-type horizontal separator designed for processing Gullfaks-A. The separation performance of this separator was validated by CFD simulations. Considering the quality of the grid system (Table 2), a negligible fraction of cells (approximately 0.0014%) have poor quality for this case. Having set all the CFD parameters for the 1988 or future-production conditions, the number of iterations required for convergence was 6,000. Each iteration took approximately 27 seconds on a 3.20-GHz PC with 2.00 GB of RAM. Therefore, a PC run time of approximately 45 hours was required for solution of continuous-phase flow regimes. Also, an additional PC run time of approximately 3 hours was required for simulation of interactions between the discrete phase (liquid droplets) and continuous phases.

Mass-distribution analysis for 1988 production conditions led to a perfect separation efficiency of 100% for both oil and water droplets. For the future-production condition, 100% of water droplets were separated, but the separation efficiency for oil droplets was only 68.0%. Therefore, it would seem that the design would suffer from low oil-separation efficiencies with the projected increase in the water-flow rate. Using the available model for weir design for the future-production conditions, additional CFD simulations were performed. In all case studies, several parallel horizontal planes were defined inside of the vessel to record the characteristics of the droplets passing through them. Software was developed to perform an analysis on the database provided by the recording surfaces. This analysis did confirm the separation velocities provided by the simple two-phase models of Fig. 3. However, the captured data also showed that some oil droplets were not able to pass through after reaching the oil/water interface. Further studies indicated that these droplets, while bouncing near the interface along the separator, were carried out by the water phase because of its high velocity. Therefore, the existence of a "re-entrainment" phenomenon, in which a fraction of oil droplets are entrained again by the water phase at high water velocities, was observed as part of the CFD simulations.

To study this phenomenon further, additional case studies were performed at various oil- and water-flow rates using the same physical model. On the basis of the 1988 and future-production conditions, the oil- and water-flow rates were varied from their minimum values to their maximum values in 10% increments. For each case study, the oil and water droplets were injected and tracked to determine if they were carried out by the other liquid phase. The results of CFD simulations indicated that independent of the oil-flow-rate value, re-entrainment by water phase occurred at a water-flow rate of 0.1595 m^3/s. Hence, the previous lower water-flow rate of 0.1329 m^3/s was assumed as the maximum value that would avoid re-entrainment of the oil droplets. Using the separator dimensions, the maximum water velocity was calculated to be 0.063 m/s. On the basis of the maximum water-production rate, a minimum cross-sectional area of 5.485 m^2 was calculated for water phase to avoid re-entrainment of the oil droplets.

Using all the data provided by the CFD simulations, the "stabilized" optimum separator was then designed using the procedure of Monnery and Svrcek (1994), and the performance of this separator was checked using CFD simulations. Fig. 2c presents the dimensions of the "stabilized" separator, and **Fig. 4** provides the detailed fluid-flow profiles for the stabilized optimum Gullfaks-A separator at the increased-water-flow-rate conditions. Again, Table 2 does indicate that only a negligible fraction of cells, approximately 0.0015%, is of poor quality for this case. As expected, a perfect separation efficiency of 100% was calculated for the oil and water droplets at both production conditions for the stabilized separator. Therefore, this design can be referred to as the realistic optimum separator for the Gullfaks-A process.

Discussion

In summary, three different separators were redesigned for Gullfaks-A. The first separator design, labeled redesigned separator, was based on the acceptable separation performance of the separator at 1988 production conditions. The originally installed separator had a reasonable separation efficiency of 98.0% for the 1988 production conditions. Hence, it was assumed that the provided retention times of continuous phases in 1988 might be necessary for a new design. Using the maximum fluid-flow rates, the separator was redesigned. The separation performance of this separator, as demonstrated by CFD simulations, was acceptable, but the design suffered from being oversized. The second separator, labeled weir

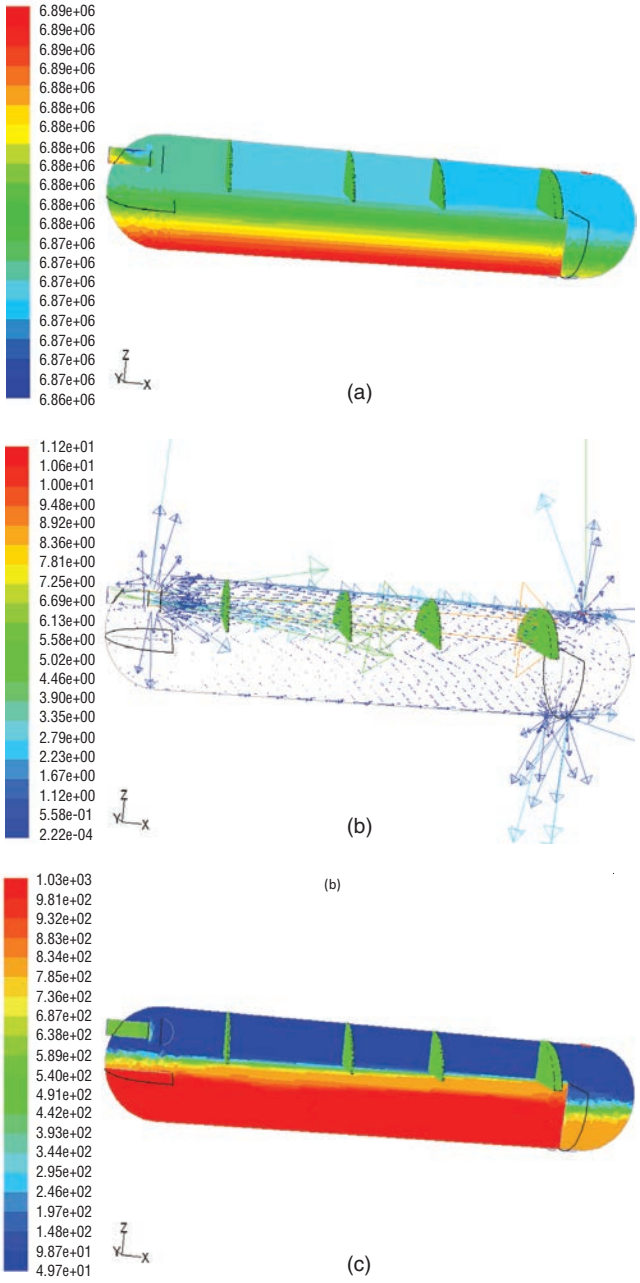

Fig. 4—Fluid-flow profiles in the middle of the stabilized separator designed for Gullfaks-A in the future-production conditions: (a) contours of pressure (Pa), (b) vectors of velocity (m/s), and (c) contours of density (kg/m^3).

design procedure used the separation velocities and interface-residence times obtained from the CFD simulations. Again, the maximum flow rates of the produced gas, oil, and water phases were used in the design.

Fig. 2b. presents the dimensions of the weir-type horizontal separator designed for processing Gullfaks-A. The separation performance of this separator was validated by CFD simulations. Considering the quality of the grid system (Table 2), a negligible fraction of cells (approximately 0.0014%) have poor quality for this case. Having set all the CFD parameters for the 1988 or future-production conditions, the number of iterations required for convergence was 6,000. Each iteration took approximately 27 seconds on a 3.20-GHz PC with 2.00 GB of RAM. Therefore, a PC run time of approximately 45 hours was required for solution of continuous-phase flow regimes. Also, an additional PC run time of approximately 3 hours was required for simulation of interactions between the discrete phase (liquid droplets) and continuous phases.

Mass-distribution analysis for 1988 production conditions led to a perfect separation efficiency of 100% for both oil and water droplets. For the future-production condition, 100% of water droplets were separated, but the separation efficiency for oil droplets was only 68.0%. Therefore, it would seem that the design would suffer from low oil-separation efficiencies with the projected increase in the water-flow rate. Using the available model for weir design for the future-production conditions, additional CFD simulations were performed. In all case studies, several parallel horizontal planes were defined inside of the vessel to record the characteristics of the droplets passing through them. Software was developed to perform an analysis on the database provided by the recording surfaces. This analysis did confirm the separation velocities provided by the simple two-phase models of Fig. 3. However, the captured data also showed that some oil droplets were not able to pass through after reaching the oil/water interface. Further studies indicated that these droplets, while bouncing near the interface along the separator, were carried out by the water phase because of its high velocity. Therefore, the existence of a "re-entrainment" phenomenon, in which a fraction of oil droplets are entrained again by the water phase at high water velocities, was observed as part of the CFD simulations.

To study this phenomenon further, additional case studies were performed at various oil- and water-flow rates using the same physical model. On the basis of the 1988 and future-production conditions, the oil- and water-flow rates were varied from their minimum values to their maximum values in 10% increments. For each case study, the oil and water droplets were injected and tracked to determine if they were carried out by the other liquid phase. The results of CFD simulations indicated that independent of the oil-flow-rate value, re-entrainment by water phase occurred at a water-flow rate of 0.1595 m^3/s. Hence, the previous lower water-flow rate of 0.1329 m^3/s was assumed as the maximum value that would avoid re-entrainment of the oil droplets. Using the separator dimensions, the maximum water velocity was calculated to be 0.063 m/s. On the basis of the maximum water-production rate, a minimum cross-sectional area of 5.485 m^2 was calculated for water phase to avoid re-entrainment of the oil droplets.

Using all the data provided by the CFD simulations, the "stabilized" optimum separator was then designed using the procedure of Monnery and Svrcek (1994), and the performance of this separator was checked using CFD simulations. Fig. 2c presents the dimensions of the "stabilized" separator, and **Fig. 4** provides the detailed fluid-flow profiles for the stabilized optimum Gullfaks-A separator at the increased-water-flow-rate conditions. Again, Table 2 does indicate that only a negligible fraction of cells, approximately 0.0015%, is of poor quality for this case. As expected, a perfect separation efficiency of 100% was calculated for the oil and water droplets at both production conditions for the stabilized separator. Therefore, this design can be referred to as the realistic optimum separator for the Gullfaks-A process.

Discussion

In summary, three different separators were redesigned for Gullfaks-A. The first separator design, labeled redesigned separator, was based on the acceptable separation performance of the separator at 1988 production conditions. The originally installed separator had a reasonable separation efficiency of 98.0% for the 1988 production conditions. Hence, it was assumed that the provided retention times of continuous phases in 1988 might be necessary for a new design. Using the maximum fluid-flow rates, the separator was redesigned. The separation performance of this separator, as demonstrated by CFD simulations, was acceptable, but the design suffered from being oversized. The second separator, labeled weir

TABLE 4—THE KEY GEOMETRIC SPECIFICATIONS AND SEPARATION EFFICIENCIES FOR VARIOUS DESIGNS PROPOSED FOR GULLFAKS-A

	Geometric Specifications					Separation Efficiency	
			Layer Thickness (m)				
Design	D (m)	L (m)	Oil Phase	Water Phase	Gravity Separation Length (m)	1988	Future
Original	3.328	16.301	1.0390	0.6250	10.216	98.0%	70.4%
Redesigned	4.845	32.081	1.6300	1.6300	25.830	99.1%	99.7%
Weir	3.48	18.37	0.9525	0.9525	12.290	100%	90.4%
Stabilized	3.84	18.40	0.6000	1.9300	12.316	100%	100%

design, was designed on the basis of the data provided by CFD simulations and the two-phase models. Although this separator was smaller than the redesigned separator, its separation efficiency was also lower.

Further CFD studies indicated that this inefficiency was caused by water-phase re-entrainment. Using the data from the two-phase models with the re-entrainment findings, the third separator, labeled stabilized separator, was designed for Gullfaks-A. This design took advantage of all phase-separation data provided by CFD simulations as well as the logical optimization methodology presented by Monnery and Svrcek (1994). The separation performance of the stabilized separator and its smaller dimensions compared with those of the redesigned separator confirmed that the redesigned separator was oversized and that a more-economical separator could be designed that could accomplish the separation task of Gullfaks-A. For comparison purposes, **Table 4** shows the key dimensions and separation efficiencies for the original, redesigned, weir, and stabilized separators proposed for Gullfaks-A.

Conclusions

Various approaches to overcoming the separation inefficiencies in a large-scale three-phase separator have been studied. The CFD-modeling strategies used for simulation of this separator resulted in a realistic simulation of its separation performance at both 1988 and future-production conditions. Therefore, the same strategies were used to verify the separation performance of the alternative case studies from a CFD-simulation perspective. The CFD simulations showed that minor adjustments could not mitigate the separation inefficiencies. Therefore, redesign of the separator was the only reasonable solution.

To accomplish this redesign task, two approaches were used. In the first approach, the separator was redesigned by one of the well-known classic methods. In the second approach, the same classic design method was improved using realistic separation parameters that resulted from CFD modeling. It was shown that the popular classic methods, mostly because of a lack of a useable mathematical model for estimation of droplet-separation velocities, do result in a very conservative design and would specify an extremely oversized separator for Gullfaks-A. In contrast with the classic separator-design methods, the CFD-simulation results indicated that significant residence times may be necessary for droplets to pass through the vapor/liquid or liquid/liquid interfaces. Furthermore, droplets may be affected and re-entrained by liquid phase at a high velocity. Thus, the realistic optimum separator can be specified only when all CFD findings in terms of phase-separation velocities and maximum continuous-phase velocities are taken into account in the design procedure.

Nomenclature

A = vessel cross-sectional area, L^2, m^2
A_H = vessel cross-sectional area for heavy-liquid phase, L^2, m^2
A_L = vessel cross-sectional area for light-liquid phase, L^2, m^2
A_{LLL} = surface area corresponding to low liquid level, L^2, m^2
A_V = surface area of vapor-disengagement zone, L^2, m^2
C_D = drag coefficient
d_p = particle diameter, L, μm
D = inside diameter of separator, L, m
g = gravity acceleration, L/t^2, m/s^2
H_H = thickness of heavy-liquid phase, L, m
H_L = thickness of light-liquid phase, L, m
H_{LLL} = height of low liquid level, L, m
H_V = height of vapor-disengagement zone, L, m
L = length of separator, L, m
$L_{\min}$ = minimum length required for vapor/liquid separation, L, m
P = operating pressure, m/Lt^2, kPa
Q_H = heavy-liquid-phase-flow rate, L^3/t, m^3/s
Q_L = light-liquid-phase-flow rate, L^3/t, m^3/s
Q_V = vapor-phase-flow rate, L^3/t, m^3/s
t_{HL} = separation time for heavy-liquid droplets from light-liquid phase, t, seconds
t_{LH} = separation time for light-liquid droplets from heavy-liquid phase, t, seconds
U_d = separation velocity of dispersed phase, L/t, m/s
V_H = holdup volume, L^3, m^3
V_S = surge volume, L^3, m^3
V_V = velocity of vapor phase, L/t, m/s
ϕ = liquid-dropout time from vapor phase, t, seconds
μ_c = continuous-phase viscosity, m/Lt, Pa·s
ρ_c = continuous-phase density, m/L^3, kg/m^3
ρ_d = dispersed-phase density, m/L^3, kg/m^3

Subscripts

c = continuous
d = dispersed, a diameter
D = drag
H = heavy liquid, holdup
L = light liquid
LLL = low liquid level
p = particle
S = surge
V = vapor
W = water

References

Abernathy, M.W.N. 1993. Gravity Settlers, Design. In *Unit Operations Handbook*, ed. J.J. McKetta Jr., 127–136. New York: Marcel Dekker.

ANSYS. 2006a. Fluent 6.3.26 software, http://www.ansys.com/Products/Simulation+Technology/Fluid+Dynamics/ANSYS+FLUENT.

ANSYS. 2006b. Gambit, version 2.4.6 (primary pre-processor for Fluent). Canonsburg, Pennsylvania: ANSYS Inc.

GPSA. 1998. *GPSA Engineering Data Book*, eleventh edition, Vol. 2, 23-2–22-3. Tulsa, Oklahoma: Gas Processors Suppliers Association.

Green, D.W. and Perry, R.H. 2008. *Perry's Chemical Engineers' Handbook*, eighth edition. New York: McGraw-Hill.

TABLE A-1—THE ASPECT-RATIO VALUES SUGGESTED BY MONNERY AND SVRCEK (1994) FOR MULTIPHASE SEPARATORS

P (kPa)	0–1700	1700–3400	0 > 3400
Aspect Ratio (*L* / *D*)	1.5–3	3–4	4–6

Grødal, E.O. and Realff, M.J. 1999. Optimal Design of Two- and Three-Phase Separators: A Mathematical Programming Formulation. Paper SPE 56645 presented at the SPE Annual Technical Conference and Exhibition, Houston, 3–6 October. http://dx.doi.org/10.2118/56645-MS.

Hansen, E.W.M., Heitmann, H., Laska, B., and Loes, M. 1993. Numerical Simulation of Fluid Flow Behavior Inside, and Redesign of a Field Separator. *Proc.,* 6th International Conference on Multiphase Production, Cannes, France, 19–21 June, 117–129.

Hooper, W.B. 1997. Decantation. In *Handbook of Separation Techniques for Chemical Engineers*, third edition, ed. P.A. Schweitzer, Part 1, Section 1.11 519–529. New York: McGraw-Hill.

Lu, Y., Lee, J.M., Phelps, D., and Chase, R. 2007. Effect of Internal Baffles on Volumetric Utilization of an FWKO--A CFD Evaluation. Paper SPE 109944 presented at the SPE Annual Technical Conference and Exhibition, Anaheim, California, USA, 11–14 November. http://dx.doi.org/10.2118/109944-MS.

Lyons, W.C. and Plisga, G.J. 2005. *Standard Handbook of Petroleum and Natural Gas Engineering*, second edition. Burlington, Massachusetts: Gulf Professional Publishing.

Monnery, W.D. and Svrcek, W.Y. 1994. Successfully Specify Three-Phase Separators. *Chem. Eng. Prog.* **90** (9): 29–40.

Monnery, W.D. and Svrcek, W.Y. 2000. Analytical Study of Liquid/Vapour Separation Efficiency. Technical Report, Petroleum Technology Alliance Canada (PTAC), Calgary, Alberta (5 September 2000), 1–20.

Pourahmadi Laleh, A. 2010. *CFD Simulation of Multiphase Separators*. PhD dissertation, University of Calgary, Calgary, Alberta, Canada (September 2010).

Pourahmadi Laleh, A., Svrcek, W.Y., and Monnery, W.D. 2012. Computational Fluid Dynamics-Based Study of an Oilfield Separator. Part I: A Realistic Simulation. *Oil and Gas Facilities* **1** (6): 57–68. http://dx.doi.org/10.2118/161212-PA.

Svrcek, W.Y. and Monnery, W.D. 1993. Design Two-Phase Separators within the Right Limits. *Chem. Eng. Prog.* **89** (10): 53–60.

Walas, S.M. 1990. *Chemical Process Equipment Selection and Design*. Newton, Massachusetts: Butterworth-Heinemann Series in Chemical Engineering, Butterworth-Heinemann.

Appendix A

This appendix provides the approach and the main steps proposed by Monnery and Svrcek (1994) for designing the optimum weir-type three-phase separator. In their design approach, droplet-settling theory is used for evaluation of phase-separation velocities. Furthermore, the economical aspect ratio of a separator (defined as the ratio of length to diameter in a separator, *L*/*D*) is assumed to be between 1.5 and 6, with a functionality of operating pressure as presented in **Table A-1.**

Separation of liquid droplets from gas phase is described by settling theory because the terminal velocity of a small droplet in a gas phase is governed by Newton's equation (Green and Perry 2008), Eq. A-1:

$$U_d = \sqrt{\frac{4\times10^{-6} g d_p (\rho_d - \rho_c)}{3 C_D \rho_c}}, \quad \text{..... (A-1)}$$

where U_d is settling velocity in m/s, g is gravity acceleration in m/s^2; d_p is droplet diameter in μm; ρ_d and ρ_c are dispersed-phase (liquid) and continuous-phase (vapor) densities; respectively, in kg/m^3; and C_D is drag coefficient, which can be calculated on the basis of the GPSA (1998) approach by means of Eqs. A-2 and A-3 (Monnery and Svrcek 2000):

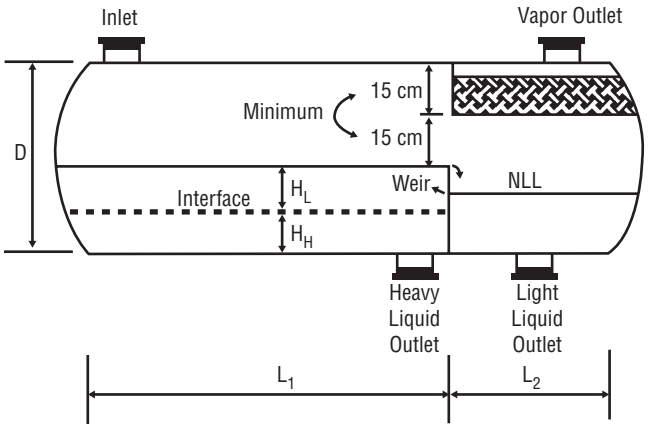

Fig. A-1—The weir design of a horizontal three-phase separator.

$$C_D = \frac{5.0074}{\ln(x)} + \frac{40.927}{\sqrt{x}} + \frac{44.07}{x}, \quad \text{..... (A-2)}$$

$$x = \frac{3.35\times10^{-9} \rho_c (\rho_d - \rho_c) d_p^{\,3}}{\mu_c^{\,2}}, \quad \text{..... (A-3)}$$

where μ_c is viscosity of continuous phase (vapor) in Pa·s.

Stokes' law is used to determine the settling or rising velocity of the droplets in liquid/liquid separation (Green and Perry 2008):

$$U_d = \frac{d_p^2 g (\rho_d - \rho_c)}{18\times10^{12} \mu_c}, \quad \text{..... (A-4)}$$

where U_d is settling (or rising) velocity in m/s; d_p is droplet diameter in μm; g is gravity acceleration in m/s^2; ρ_d and ρ_c are dispersed-phase and continuous-phase densities, respectively, in kg/m^3; and μ_c is continuous-phase viscosity in Pa·s. Abernathy (1993) and Monnery and Svrcek (1994) proposed that a maximum practical-separation velocity of 0.00423 m/s be used as an upper limit in Eq. A-4. The droplet size of 150 μm has been used as a standard in the API design method (Walas 1990; Hooper 1997).

To determine the most-economical separator, an iterative design procedure is required. **Fig. A-1** shows the design parameters for a weir-type separator. First, the terminal settling velocity of oil droplets is estimated using Eq. A-1, and vapor velocity is set to be equal to 75% of the terminal settling velocity. Then, holdup and surge volumes (V_H and V_S, respectively) are calculated on the basis of given holdup and surge times and volumetric flow rate of light liquid (Q_L). The other steps are outlined in the following:

1. Pick an aspect ratio from Table A-1 and calculate the initial vessel diameter:

$$D = \sqrt[3]{\frac{16(V_H + V_S)}{0.6\pi\left(\frac{L}{D}\right)}}, \quad \text{..... (A-5)}$$

2. Calculate the vessel cross-sectional area:

$$A = \frac{\pi D^2}{4}, \quad \text{..... (A-6)}$$

3. Set H_V to the larger of (0.20× D) or 0.60 m, and then calculate A_V.

4. Set the low liquid level (H_{LLL}) in the light-liquid section, and then calculate A_{LLL}.

5. Calculate the weir height:

$$H_W = D - H_V, \quad \text{..... (A-7)}$$

If $H_W < 60$ cm, then increase D and go to Step 2.

6. Calculate L_2 on the basis of the light-liquid holdup/surge:

$$L_2 = \frac{V_H + V_S}{A - A_V - A_{LLL}}, \quad \text{..... (A-8)}$$

7. Set the interface at $\frac{H_W}{2}$ (typical setting) and obtain H_H and H_L.

8. Using the H_H value, calculate A_H and set $A_L = A - A_V - A_H$.

9. Calculate the separation velocities of liquid phases using Stokes' law (Eq. A-4).

10. Calculate the separation times of the liquid droplets (t_{HL} and t_{LH}).

11. Set the larger of $\frac{t_{LH} Q_H}{A_H}$ and $\frac{t_{HL} Q_L}{A_L}$ as the required length for liquid/liquid separation (L_1).

12. Set $L = L_1 + L_2$.

13. Calculate the liquid-dropout time:

$$\phi = \frac{H_V}{V_V}, \quad \text{..... (A-9)}$$

14. Calculate the actual vapor velocity using Q_V and A_V.

15. Calculate the minimum length required for vapor/liquid separation ($L_{\min}$) using the actual vapor velocity and the liquid-dropout time.

16. If $L < 0.8L_{\min}$, then increase H_V and go to Step 3. If $L < L_{\min}$, then set $L = L_{\min}$. If $L > 1.2L_{\min}$, then decrease H_V (if acceptable) and go to Step 3. Otherwise, L is acceptable.

17. If $\frac{L}{D} < 1.5$, then decrease D (if acceptable) and go to Step 2. If $\frac{L}{D} > 6$, then increase D and go to Step 2.

18. Calculate the approximate vessel weight on the basis of the thickness and the surface area of the shell and heads.

19. To find the optimum case (corresponding to the minimum weight), change the vessel diameter by 15-cm increments and repeat the calculations from Step 2, while keeping the aspect ratio in the range of 1.5 to 6.0.

Ali Pourahmadi Laleh is a research engineer with the Reservoir Simulation Group in Calgary. He has more than 11 years of experience as a research engineer, involved in rectifying industrial-scale process inefficiencies and optimizing chemical plants. Pourahmadi Laleh has conducted research in separation technologies, coal liquefaction, and in-situ upgrading by hot-fluid injection. He has proposed a novel approach for automatic design of the optimum distillation-column sequence using genetic algorithms, and he has also developed an efficient strategy for realistic simulation of oilfield separators, providing improved design criteria for these multiphase separators. Pourahmadi Laleh holds a BS degree from Sahand University of Technology, an MS degree from Sharif University of Technology, and a PhD degree from the University of Calgary, all in chemical engineering.

William Y. Svrcek is a professor emeritus at the University of Calgary and president of Virtual Materials Group in Calgary. Before joining the University of Calgary, he worked for Monsanto Company as a senior systems engineer and as an associate professor (1970–75) at the University of Western Ontario. Svrcek was also a senior partner in Hyprotech, now part of Aspen Technology, from its incorporation in 1976. As a principal, director, and president (1981–1993), he was instrumental in establishing Hyprotech as a leading international process-simulation software company. Svrcek's teaching and research interests center on process simulation control and design. He has been involved for many years in teaching the continuing-education course titled "Computer-Aided Process Design—Oil and Gas Processing," which has been presented worldwide. Svrcek has authored or coauthored more than 200 technical articles/reports and has supervised more than 50 graduate students. He holds BS and PhD degrees in chemical engineering from the University of Alberta.

Wayne D. Monnery is president of Chem-Pet Process Tech Limited in Calgary and is an adjunct associate professor at the University of Calgary. He has 24 years of industrial experience as a process engineer, with recognized expertise in applied thermodynamics, in process simulation and physical properties of petroleum systems, and in sweet-gas processing, sour-gas treating, and sulfur recovery. Monnery has also worked on heavy-oil and steam-assisted gravity-drainage facility simulation and design. He has conducted research in sulfur-plant kinetics, alternative sour-gas treating, water content of high-pressure acid gases for acid-gas injection, and phase separation. Monnery holds a PhD degree in chemical engineering from the University of Calgary.